Geomechanics and Engineering, *Vol. 13, No. 4 (2017) 701-714*
DOI: https://doi.org/10.12989/gae.2017.13.4.701

Uplift capacity of horizontal anchor plate embedded near to the cohesionless slope by limit analysis

Paramita Bhattacharya* and Sagarika Sahoo[a]

Department of Civil Engineering, Indian Institute of Technology Kharagpur, Kharagpur 721302, India

(*Received August 3, 2016, Revised April 5, 2017, Accepted May 8, 2017*)

Abstract. The effect of nearby cohesionless sloping ground on the uplift capacity of horizontal strip plate anchor embedded in sand deposit with horizontal ground surface has been studied numerically. The numerical analysis has been carried out by using the lower bound theorem of limit analysis with finite elements and linear optimization. The results have been presented in the form of non-dimensional uplift capacity factor of anchor plate by changing its distance from the slope crest for different slope angles, embedment ratios and angles of soil internal friction. It has been found that the decrease in horizontal distance between the edge of the anchor plate and the slope crest causes a continuous decrease in uplift capacity of anchor plate. The optimum distance is that distance between slope crest and anchor plate below which uplift capacity of an anchor plate has been found to decrease with a decrease in normalized crest distance from the anchor plate in presence of nearby sloping ground. The normalized optimum distance between the slope crest and the anchor plate has been found to increase with an increase in slope angle, embedment ratio and soil internal friction angle.

Keywords: strip anchor; uplift capacity; limit analysis; finite elements; cohesionless slope

1. Introduction

Anchors are often used as the sub-structural tensile members that transmit the tensile force from the superstructure to the surrounding soil. The shear strength of the surrounding soil is used to resist this uplift force. Examples of such structures include transmission towers, dry-dock, submerged pipelines, tunnels etc. A number of research investigations have been performed by many researchers following different approaches to estimate the uplift capacity of anchors embedded in homogeneous sand deposit or layered sand deposit. These different approaches are: (1) the limit equilibrium method (Meyerhof and Adams 1968, Meyerhof 1973, Rangari *et al*. 2013), (2) the method of stress characteristics (Rao and Kumar 1994), (3) the elasto-plastic finite element analysis (Rowe and Davis 1982, Sakai and Tanaka 2007, Andresen *et al*. 2011, Bildik *et al*. 2013, Niroumand and Kassim 2014a, b, c, Keskin 2015), (4) the upper bound limit analysis (Kumar 1997, 2001, 2003, Merifield and Sloan 2006, Kumar and Kouzer 2008, Yu *et al*. 2014), (5) the lower bound limit analysis (Basudhar and Singh 1994, Merifield and Sloan 2006, Merifield *et al*. 2006, Khatri and Kumar 2011, Bhattacharya and Kumar 2014, 2016); (6) 1-g small scale laboratory model tests (Das and Seeley 1975, Murray and Geddes 1987, Bouazza and Finlay 1990,

*Corresponding author, Assistant Professor, E-mail: paramita@civil.iitkgp.ernet.in
[a]M.Tech. Student, E-mail: lilysagarika@gmail.com

http://www.techno-press.org/?journal=gae&subpage=7 ISSN: 2005-307X (Print), 2092-6219 (Online)

akai and Tanaka 2007, Niroumand and Kassim 2014a, b, c, Keskin 2015) and (7) centrifuge model tests (Ovesen 1981, Dickin 1988). Except the investigations carried out by Kumar (1997), Bildik *et al*. (2013) and Yu *et al*. (2014) most of the research investigations determined the uplift capacity of the horizontal anchor plate embedded in sand with horizontal ground surface.

Kumar (1997) investigated the pullout capacity of strip anchor plate embedded in sandy slope by using upper bound limit analysis with an assumed failure mechanism where anchor plate was placed horizontally and parallel to the inclined ground surface. Bildik *et al*. (2013) performed finite element analysis with usage of an elasto-plastic hyperbolic model named as Hardening Soil Model (HSM) in PLAXIS. The analysis was performed for three different embedment ratios, say H/B equal to 2, 5 and 8 for soils of different relative densities where H and B are embedment depth and width of the anchor plate, respectively. Bildik *et al*. (2013) studied the effect of nearby slope on the uplift capacity of anchor plate placed at the crest of the slope (i.e., $s/B = 0$ where s is the distance between slope crest and nearest edge of the anchor plate of width B) considering different values of slope angle and wide range of soil friction angle. The variation of reduction of uplift capacity with non-dimensional crest distance was reported up to $s/B = 5$ and for one slope angle. No discussion was made on (i) the optimum crest distance where uplift capacity becomes free from the effect of the nearby sloping ground; and (ii) the effect of slope angle on this optimum non-dimensional crest distance. Yu *et al*. (2014) have used three upper bound approaches, say upper bound mechanism, block set mechanism and numerical upper bound limit analysis with finite elements to determine the pullout capacity of anchors embedded in sandy slopes and studied the effect of embedment ratio, slope angle and anchor inclination on the pullout capacity of anchor.

From the literature it is understood that there is a gap in the study of the uplift capacity of the horizontal anchor plate embedded in sand near to sloping ground to determine the optimum distance between anchor plate and slope crest for different type of sands and for different embedment depth. The position of the anchor plate relative to the position of nearby sloping ground plays an important role and may vary with different values of slope angle and the soil friction angle.

In the present work, an attempt has been made to determine the uplift capacity of strip anchor plate located near the cohesionless slope by employing lower bound theorem of limit analysis with finite elements and linear programming. The lower bound solution can be used in the design related problems to find out safe estimate of the ultimate bearing capacity of foundations (Sloan 1988, Lyamin and Sloan 2002, Kumar and Khatri 2008) and ultimate uplift capacity of anchors (Merifield and Sloan 2006, Merifield *et al*. 2006, Bhattacharya and Roy 2016). The main objective of the present work is to study the effect of the presence of sandy slope on the uplift capacity of horizontal anchor plate embedded in horizontal ground surface nearby the cohesionless slope and to determine the optimum distance (s_{opt}) between slope crest and the anchor plate where the effect of nearby slope does not cause any reduction in anchor's uplift capacity. It is achieved by varying the position of the anchor plate relative to the position of the slope crest up to the distance where no effect of the sloping ground is observed. The effects of the distance between the anchor plate and slope crest (s) and the angle of the slope (β) have been studied for different embedment ratios (H/B) ranging from 3 to 7 and different angles of soil internal friction (ϕ), namely 30°, 35°, 40° and 45°. The failure patterns have also been studied for anchor plate placed near to the sandy slope.

2. Problem definition

A strip anchor plate of width B is embedded horizontally in cohesionless soil medium with

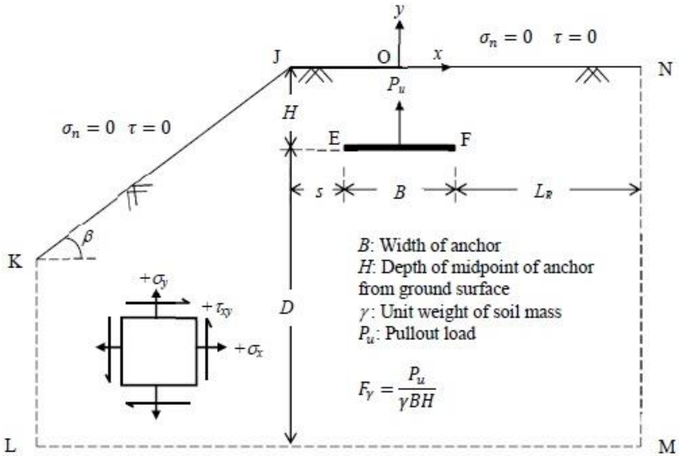

Fig. 1 Schematic diagram of the problem

horizontal ground surface near to a sandy slope. The thickness of the anchor plate is assumed to be negligible compared to its width (*B*). β is the slope angle of the nearby sloping ground with respect to the horizontal surface as shown in Fig. 1. The anchor plate is placed at a depth of *H*, measured vertically from the horizontal ground surface. The distance between the crest of the sloping ground and the nearest end of the plate from the crest is assumed to be *s* which varies from 0 to 11*B*. It is to determine the magnitude of the collapse load, P_u per unit length of the plate where the direction of pullout is kept perpendicular to the plate. The soil medium is assumed to follow the Mohr-Coulomb failure criterion and an associated flow rule. The magnitude of P_u is determined for different values of embedment ratio (*H*/*B*), angle of soil friction (ϕ), slope angle (β) and distance between the slope crest and the anchor plate (*s*). The interface friction angle between the anchor plate and adjoining soil mass (δ) is kept equal to ϕ.

2.1 Domain, finite element mesh and stress boundary conditions

The problem domain JKLMN, as shown in Fig. 1, is chosen for the analysis. In this domain JK represents the slope with a slope angle β and JN represents the horizontal ground surface near to the slope. The anchor plate is placed along the horizontal line EF. The horizontal distance (*s*) between the slope crest and the left edge of the anchor plate is varied between 0 and 11*B* depending on the values of ϕ, *H*/*B* and β. The horizontal distance (L_R) between the right edge of the anchor plate and the vertical boundary NM is varied between 20*B* and 150*B* whereas the vertical distance (*D*) between the horizontal anchor plate (EF) and the bottom boundary (LM) of the domain is varied between 4*B* and 18*B* such that the yielded elements do not approach towards right and bottom boundaries of the chosen domain and its further increase in size does not affect the magnitude of the collapse load.

The stress boundary conditions that are imposed in the analysis are shown in the Fig. 1. The values of normal (σ_n) and shear (τ) stresses are equal to zero along the stress free both horizontal as well as sloping ground surfaces NJ and JK, respectively. Along the top and bottom interfaces between the anchor plate and the surrounding soil, the following stress boundary condition is imposed

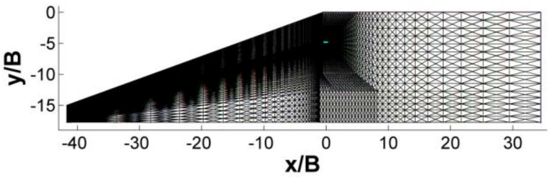

N = 47700 E = 15900 D_c = 23732 N_i = 18

(a)

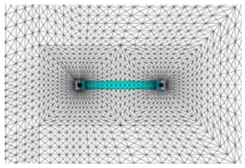

Zoomed view around anchor plate plate for H/B = 5, β = 20° and s/B = 0

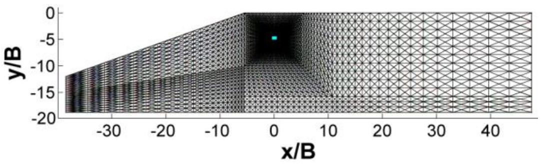

N = 37968 E = 12656 D_c = 18882 N_i = 18

(b)

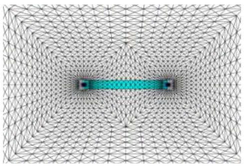

Zoomed view around anchor plate plate for H/B = 5, β = 20° and s/B = 5

Fig. 2 Typical finite element meshes for anchor plate embedded at H/B = 5 nearby a slope of β = 20° with (a) s/B = 0 and (b) s/B = 5

$$|\tau_{xy}| \leq (-\sigma_y) \tan \delta \tag{1}$$

Here σ_y represents the normal stress acting on the anchor-soil interfaces and the negative sign with σ_y is used as the tensile stresses are considered to be positive in the analysis. The sign convention followed for this analysis is also presented in Fig. 1.

The chosen domain is discretized into a number of three noded triangular elements. The sizes of the elements are chosen in a way such that sizes are decreased towards the edges of the anchor plate. Typical finite element meshes for H/B = 5, ϕ = 30° and β = 20° with s/B = 0 and 5 are shown in Fig. 2 where N, E and D_c represents the total number of nodes, elements and stress discontinuities, respectively. The values of N, E and D_c increases with increase in values of H/B, ϕ and β.

3. Analysis

3.1 Numerical formulation for lower bound limit analysis with finite elements

The lower bound limit analysis in combination with finite elements and linear programming has been performed to determine the uplift capacity of strip anchor. The methodology proposed by Sloan (1988) for the plane strain problem has been used here to perform the analysis. The nodal stresses (σ_x, σ_y and τ_{xy}) are considered as the unknown variables. The following element equilibrium conditions are satisfied everywhere in the soil domain

$$\frac{\partial \sigma_x}{\partial x} + \frac{\partial \tau_{xy}}{\partial y} = 0 \tag{2a}$$

$$\frac{\partial \tau_{xy}}{\partial x} + \frac{\partial \sigma_y}{\partial y} = \gamma \tag{2b}$$

Where γ is the unit weight of soil mass.

Statically admissible stress discontinuities are permitted along the interfaces of all the adjacent triangular elements. The continuity of shear and normal stresses are ensured along every stress discontinuity line. The following Mohr-Coulomb yield criterion are satisfied everywhere in the cohesionless soil domain

$$F = (\sigma_x - \sigma_y)^2 + 4\tau_{xy}^2 - [-(\sigma_x + \sigma_y)\sin\phi]^2 = 0 \tag{3}$$

The original Mohr-Coulomb yield function was linearized by a regular polygon of *p*- sides inscribed in the parent yield circle (Bottero *et al*. 1980) in order to use linear programing. The value of *p* has been taken equal to 21 following Kumar and Khatri (2008). The magnitude of the collapse load P_u per unit length of the anchor plate is determined by integrating the normal stresses acting along the top and the bottom interfaces of the anchor plate by using the following expression

$$P_u = \int_{Top\ interface} (-\sigma_y dx) - \int_{Bottom\ interface} (-\sigma_y dx) \tag{4}$$

The magnitude of P_u is then maximized subjected to a set of equality and inequality linear constraints as stated below

$$\text{Maximize the objective function:} \quad -\{c\}^T\{\sigma\} \tag{5a}$$

$$\text{Subjected to (i)equality constraints:} \quad \{A_{eq}\}\{\sigma\} = \{b_{eq}\} \tag{5b}$$

$$\text{(ii) ineuqality constraints:} \quad \{A_{ineq}\}\{\sigma\} \leq \{b_{ineq}\} \tag{5c}$$

The LINPROG function available in *MATLAB R2012b* was used to perform the linear optimization.

3.2 Definition of the uplift capacity factor (F_γ)

The uplift capacity of a strip anchor plate of width *B* and embedded at a depth of *H* below the horizontal ground surface can be expressed in terms of a non-dimensional uplift capacity factor, F_γ as defined below

$$F_\gamma = \frac{P_u}{\gamma BH} \tag{6}$$

4. Results and comparison

4.1 Variation of uplift capacity factor (F_γ)

The variations of uplift capacity factor (F_γ) of horizontal anchor plate with its distance from the slope crest in non-dimensional form (s/B) are presented in Figs. 3-7 for different values of H/B, β and ϕ. Results indicate that the uplift capacity of anchor plate depends upon the normalized crest

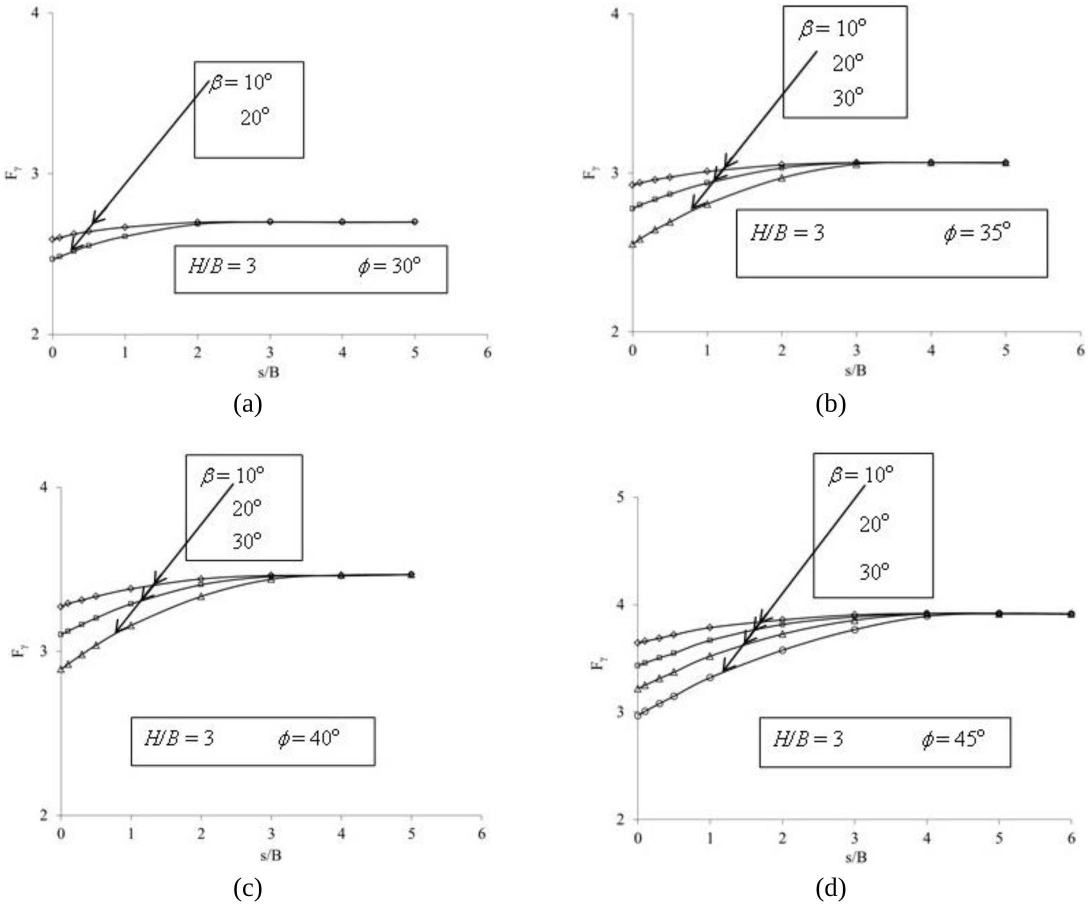

Fig. 3 Variation of F_γ with s/B for different values of β and H/B = 3 with (a) $\phi = 30°$, (b) $\phi = 35°$; (c) $\phi = 40°$ and (d) $\phi = 45°$

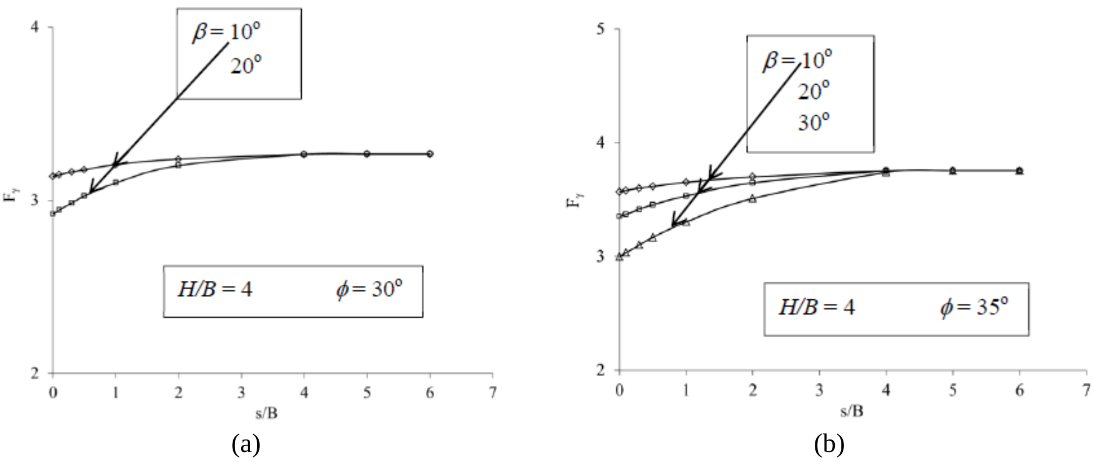

Fig. 4 Variation of F_γ with s/B for different values of β and H/B = 4 with (a) $\phi = 30°$, (b) $\phi = 35°$; (c) $\phi = 40°$ and (d) $\phi = 45°$

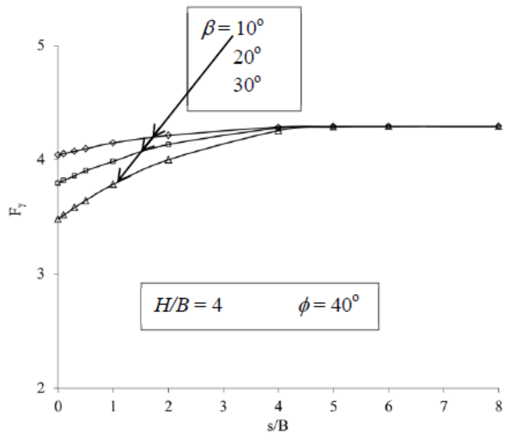

(c)

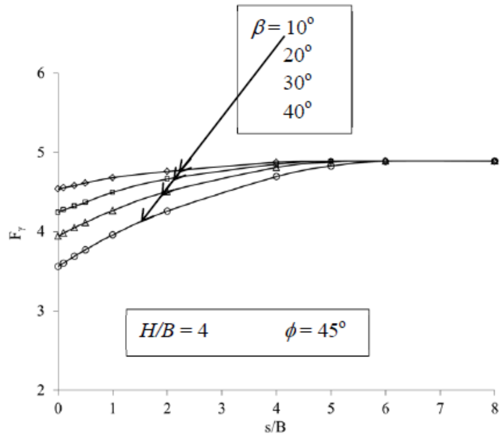

(d)

Fig. 4 Continued

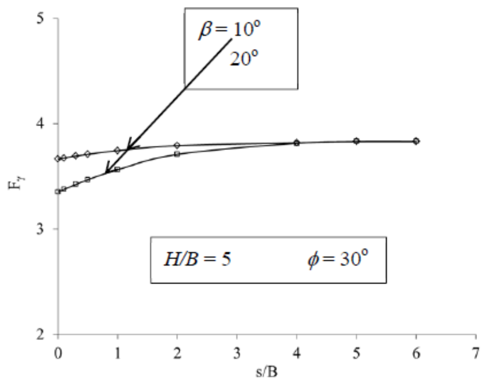

(a)

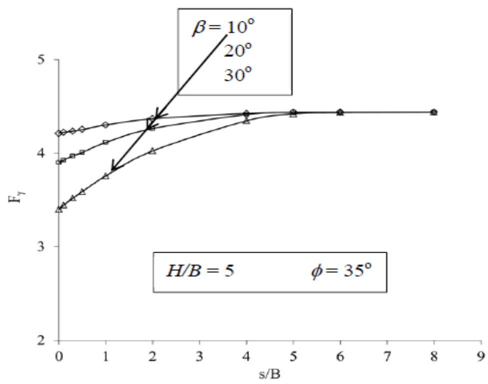

(b)

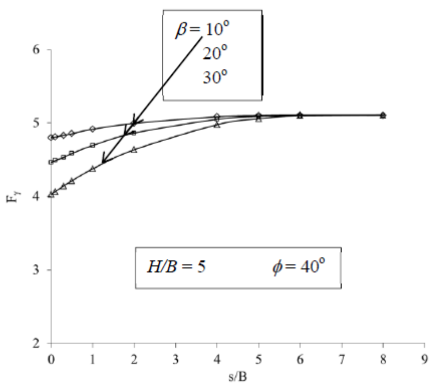

(c)

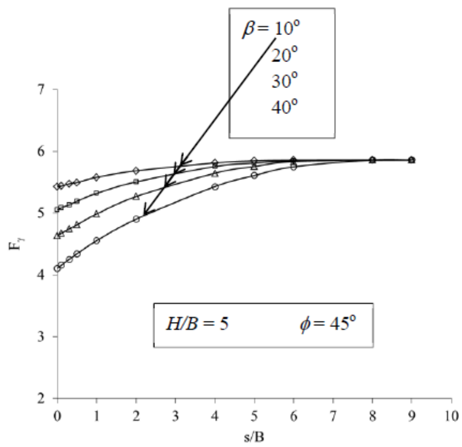

(d)

Fig. 5 Variation of F_γ with s/B for different values of β and H/B = 5 with (a) ϕ = 30°, (b) ϕ = 35°; (c) ϕ = 40° and (d) ϕ = 45°

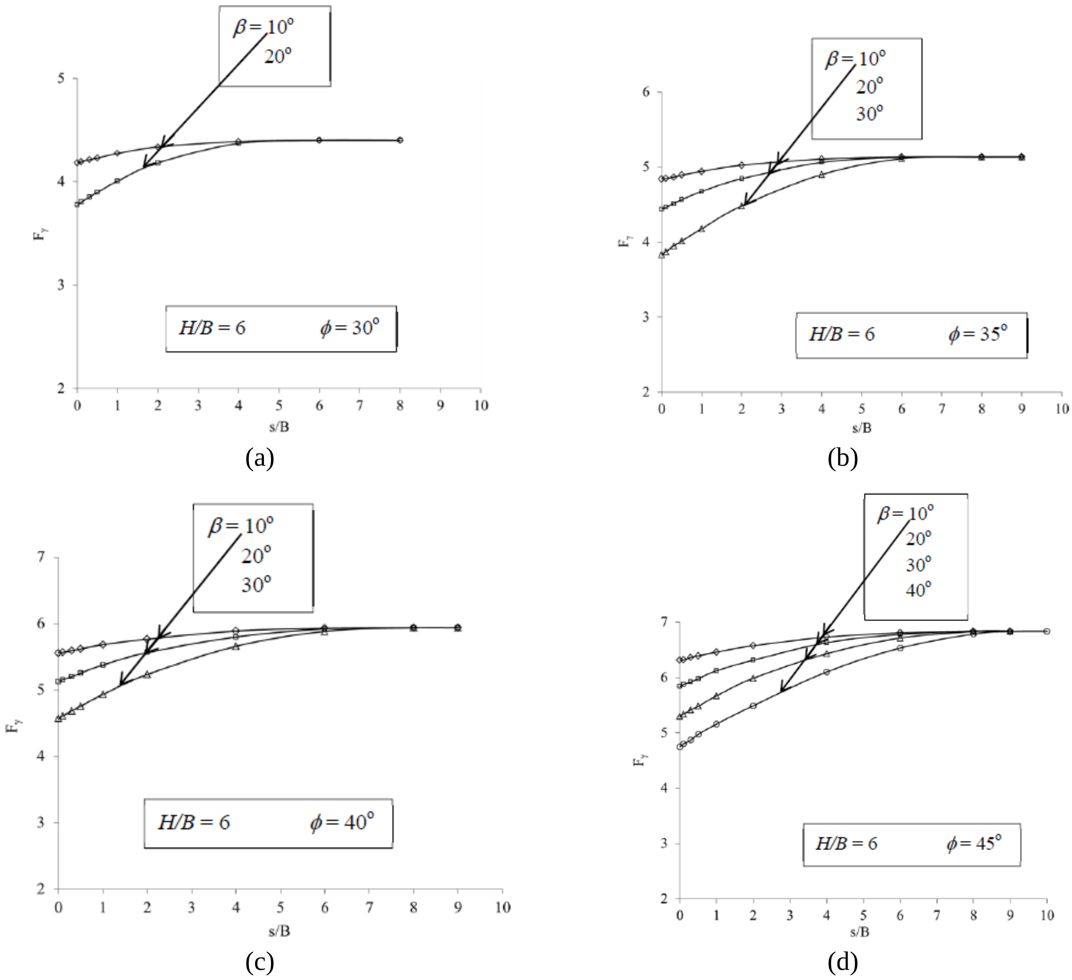

Fig. 6 Variation of F_γ with s/B for different values of β and H/B = 6 with (a) ϕ = 30°, (b) ϕ = 35°; (c) ϕ = 40° and (d) ϕ = 45°

distance (s/B), embedment ratio (H/B), inclination angle (β) of the nearby sloping ground, and soil internal friction angle (ϕ). The following observations are made from the results presented in Figs. 3-7:

• The results show that the nearby sloping ground causes a reasonable reduction in the uplift capacity of the anchor plate. The uplift capacity has been found to be minimum when the left edge of the anchor plate (which is eventually the nearest edge of the anchor plate to the slope crest) and the slope crest lie on the same vertical plane, i.e., at s/B = 0. The uplift capacity of the anchor plate increases with an increase in s/B for all values of β, H/B and ϕ. The normalized distance between the slope crest and the anchor plate at which the effect of the nearby sloping ground on the uplift capacity of the anchor plate diminishes is called the normalized optimum distance (s_{opt}/B). The maximum value of uplift capacity is equal to the uplift capacity of the anchor plate embedded in a sand deposit with horizontal ground surface in absence of any nearby sloping ground. Therefore

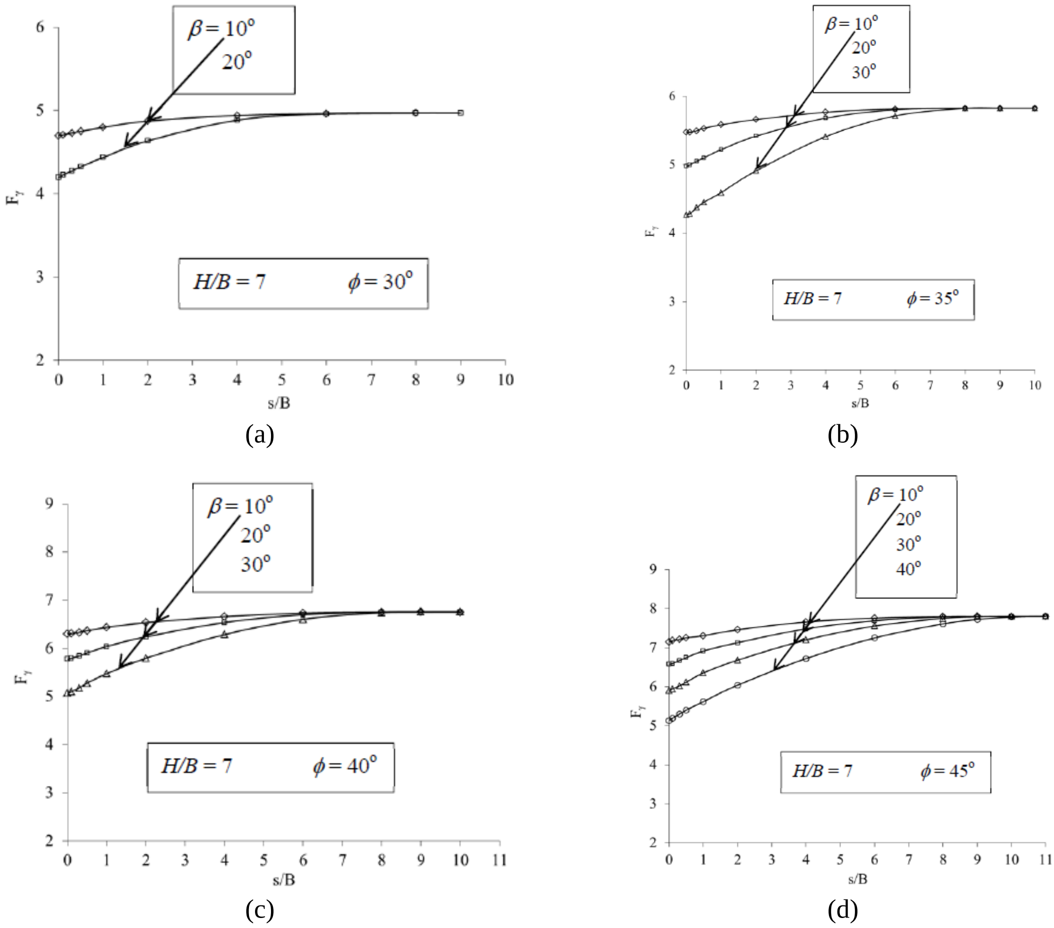

Fig. 7 Variation of F_γ with s/B for different values of β and H/B = 7 with (a) ϕ = 30°, (b) ϕ = 35°; (c) ϕ = 40° and (d) ϕ = 45°

the effect of sloping ground on the uplift capacity of the anchor plate is encountered for $0 \leq s/B < s_{opt}/B$. The values of s_{opt}/B found in Figs. 3-7 for different combinations of H/B, β and ϕ are provided in Table 1.The value of normalized optimum spacing (s_{opt}/B) has been found to be higher for higher value of slope angle (β). Similarly the normalized optimum distance (s_{opt}/B) between the slope crest and anchor plate also increases with an increase in H/B keep keeping β and ϕ are unchanged.

•The reduction in the magnitude of uplift capacity increases with an increase in slope angle (β) kept other parameters unchanged.

•For any combination of H/B and β the magnitude of the minimum value of F_γ and normalized optimum distance (s_{opt}/B) between slope crest and the anchor plate depend on the value of soil friction angle (ϕ). Minimum value of F_γ has been found to be lower for lower value of ϕ whereas s_{opt}/B has been found to be higher at higher value of ϕ for a particular combination of H/B and β.

•The uplift capacity factor (F_γ) for all values of s/B increases with an increase in H/B for any particular value of ϕ and β.

Table 1 s_{opt}/B for different combination of H/B, ϕ and β

H/B	s_{opt}/B											
	ϕ = 30°		ϕ = 35°			ϕ = 40°			ϕ = 45°			
	β = 10°	β = 20°	β = 10°	β = 20°	β = 30°	β = 10°	β = 20°	β = 30°	β = 10°	β = 20°	β = 30°	β = 40°
3	2.0	2.5	2.8	3.0	3.5	2.8	3.5	3.8	3.5	3.8	4.0	4.8
4	4.0	4.0	3.7	4.0	4.4	4.5	4.8	5.0	4.6	5.0	5.4	6.0
5	4.5	5.0	4.5	5.0	6.0	5.0	6.5	7.2	5.6	7.0	7.4	8.0
6	5.0	5.3	5.0	6.0	7.2	6.5	7.0	8.0	7.6	8.0	8.2	9.0
7	6.0	6.2	6.6	8.0	9.0	8.0	8.0	9.0	8.4	9.1	10	11.0

4.2 Comparison of F_γ for strip anchor embedded in sand

4.2.1 In absence of sloping ground nearby (β = 0°)

The present computational work has been validated by comparing the calculated F_γ value for horizontal strip anchor embedded in sand deposit at a reasonably distance (> s_{opt}) away from the sloping ground with the numerical and experimental F_γ results provided by (i) Merifield and Sloan (2006) by using upper and lower bounds solutions; (ii) Murray and Geddes (1987) by using upper bound method with an assumed failure mechanism; and (iii) Murray and Geddes (1989) by performing a series of 1-g laboratory model tests. The comparison has been presented in Fig. 8. No nearby slope was modelled or considered in the domain reported in literature to determine the F_γ values. The present numerical result matches well with the available lower bound solution (Merifield and Sloan 2006) and always lies below the upper bound solution reported in literature by Merifield and Sloan 2006 with maximum 10% difference. Maximum difference of 1% between the two lower bound solutions has been noticed at ϕ = 40°. The present lower bound solution is found to be marginally on the lower side in comparison to the upper bound solution provided by Murray and Geddes (1987) based on a straight line failure mechanism. The maximum difference between present results and the upper bound solution provided by Murray and Geddes (1987) is around 1.7%. However the experimental results based on 1-g small scale tests reported by Murray and Geddes (1989) has been found to be on the higher side of the present results with maximum difference of 15.5%.

4.2.2 In presence of sloping ground nearby ($\beta \neq$ 0°)

A comparison between present lower bound solution and the solution suggested by Bildik *et al*. (2013) based on an elasto-plastic finite element has been shown in Table 2 for three different values of slope angles, say β equals to 25°, 30° and 35° with three different values of soil friction angles at s/B = 0 and H/B = 5. The comparison is made in terms of uplift capacity reduction factor (ξ_r) defined below

$$\xi_r = \frac{(P_u)_{in\ presence\ of\ slope\ nearby}}{(P_u)_{in\ absence\ of\ slope\ nearby}} \tag{7}$$

Although the lower bound limit analysis performed here is strictly applicable for an associated flow rule material, the magnitude of the collapse load can be determined approximately (Sloan 2013) for any given value of dilatancy angle (ψ) by using the reduced shear strength parameter ϕ^* for sand. For non-associated case ($0 < \psi < \phi$), the reduced shear strength parameter ϕ^*, instead of ϕ,

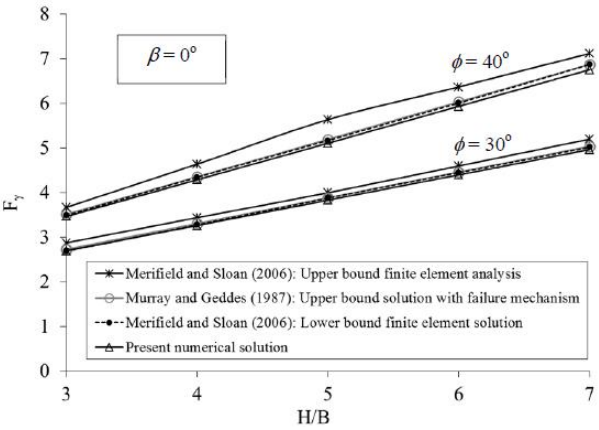

(a)

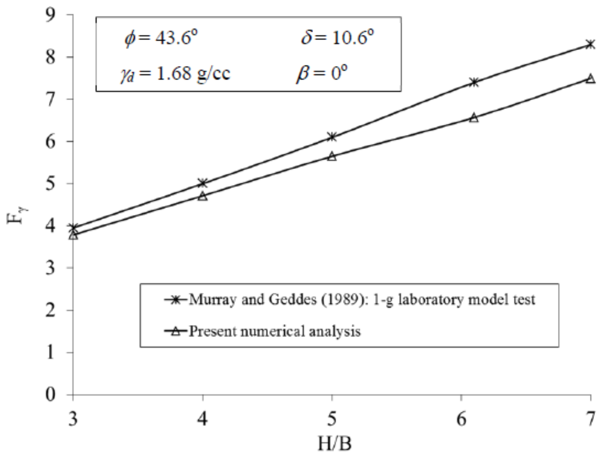

(b)

Fig. 8 Comparison of the present numerical work with (a) available numerical works and (b) available experimental work in literature

for cohesionless material can be calculated based on the expressions given by Davis (1968)

$$\tan\phi^* = \eta\tan\phi, \quad \text{where} \quad \eta = \frac{\cos\psi\cos\phi}{1-\sin\psi\sin\phi} \tag{8}$$

The reduced shear strength parameter has been calculated by using Eq. (8) for the comparison purpose and used for the present lower bound FELA and upper bound FELA reported by Yu *et al*. (2014). The trends of the present lower bound solution match well with the solution reported by Bildik *et al*. (2013) but the difference between two results are also noted. The present results for s/B = 0 with H/B = 5 match reasonably well the value reported by Yu *et al*. (2014) for the case when anchor plate is fully embedded in sandy slope. It is worthy to mention here that the uplift capacity reduction factor of the anchor plate embedded in sandy slope should be lower than the same for the anchor plate embedded in horizontal ground surface with nearby sloping ground at s/B = 0.

Table 2 Comparison of the present lower bound solution with existing works in literature

Soil friction angle	Dilatancy angle	β	Uplift capacity reduction factor (ξ_r)		
			Present lower bound analysis[1]	Bildik *et al*. (2013)[2]	Yu *et al*. (2014)[3]
35	5	25	0.855	0.68	-
		30	0.753	0.62	-
40	10	25	0.95	0.70	-
		30	0.90	0.65	
		35	0.80	0.57	
45	15	25	0.96	0.72	0.97
		30	0.91	0.66	0.92
		35	0.86	0.58	0.90

[1] Lower bound finite element analysis with the usage of reduced shear strength parameter ϕ^* calculated by Eq. (8) for anchor plate embedded in horizontal ground surface with nearby sloping ground at $s/B = 0$

[2] Elasto-plastic FEA considering dilatancy of the soil for anchor plate embedded in horizontal ground surface with nearby sloping ground at $s/B = 0$

[3] Upper bound finite element analysis with the usage of reduced shear strength parameter ϕ^* calculated by Eq. (8) for anchor plate embedded in sloping ground surface

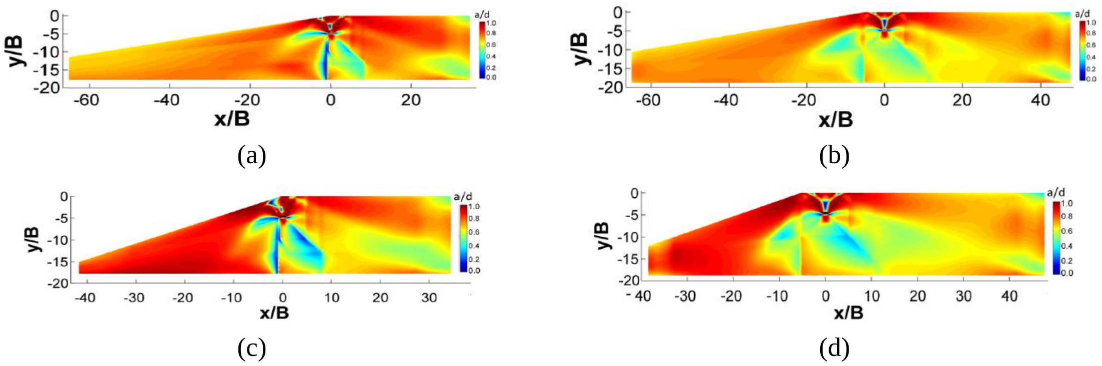

Fig. 9 Proximity of the stress state to plastic failure for anchor plate embedded in sand of $\phi = 30°$ at $H/B = 5$ with (a) $s/B = 0$ and $\beta = 10°$, (b) $s/B = 5$ and $\beta = 10°$, (c) $s/B = 0$ and $\beta = 20°$ and (d) $s/B = 5$ and $\beta = 20°$

4.3 Failure pattern

The proximity of the stress state, with respect to shear failure, in the optimized statically admissible stress field is evaluated at the centroids of each element, in terms of a/d ratio, where, $a = (\sigma_x - \sigma_y)^2 + (2\tau_{xy})^2$ and $d = [(\sigma_x + \sigma_y)\sin\phi]^2$. The proximity of the stress state to plastic failure surrounding the horizontal anchor plate embedded in sand deposit at $H/B = 5$ with horizontal ground surface are drawn for (i) $s/B = 0$ and $\beta = 10°$, (ii) $s/B = 5$ and $\beta = 10°$; (iii) $s/B = 0$ and $\beta = 20°$ and (iv) $s/B = 5$ and $\beta = 20°$. The corresponding failure patterns are shown in Fig. 9. The value of a/d becomes unity for a point to be at plastic state. A very dark red color implies a fully plastic region with $a/d = 1$.

A symmetric failure zone about the axis of the anchor plate on its both sides has been observed at $s/B = 5 \approx s_{opt}/B$ for both $\beta = 10°$ and $20°$. The symmetric failure zone starts from both the edges of the anchor plate and reaches to the horizontal ground surface. The failure zone becomes asymmetric for the same values of β (say, 10° and 20°) but when $s/B = 0$. In this case the failure patterns start from the edges of the anchor plate and incline towards the nearby sloping ground and intersect it as shown in Figs. 9(b)-9(d). In addition to this, a non-plastic zone with very low a/d value (dark blue color) has been noticed in Figs. 9(a)-9(d) immediately above the anchor plate which is symmetric and reaching up to the horizontal ground level for $s/B = 5$ but for $s/B = 0$ this non-plastic zone of dark blue color becomes asymmetric, shifted towards the sloping ground with an inclination.

5. Conclusions

The influence of nearby sandy slope in the magnitude of uplift capacity of horizontal anchor plate embedded in cohesionless soil deposit with horizontal ground surface has been investigated here. The analysis has been carried out for a wide range of embedment ratio (H/B), soil friction angle (ϕ) and the slope angle (β) of the nearby slope. From the present analysis it has been concluded that the uplift capacity of the horizontal anchor plate of width B can be reduced considerably in presence of nearby sloping ground within a normalized optimum distance (s_{opt}/B). The magnitude of reduction of anchor uplift capacity depends on the normalized distance between anchor plate and slope crest (s/B) and slope angle (β) for any combination of H/B and ϕ. However, the uplift capacity of the anchor plate may become unaffected even in the presence of sloping ground far away than the optimal distance i.e., $s/B > s_{opt}/B$.

References

Andresen, L., Jostad, P.H. and Andersen, K.H. (2011), "Finite element analysis applied in design of foundations and anchors for offshore structures", *J. Geomech.*, **11**(6), 417-430.

Basudhar, P.K. and Singh, D.N. (1994), "A generalized procedure for predicting optimal lower bound break-out factors of strip anchors", *Geotechnique*, **44**(2), 307-318.

Bhattacharya, P. and Kumar, J. (2014), "Pullout capacity of inclined plate anchors embedded in sand", *Can. Geotech. J.*, **51**(11), 1365-1370.

Bhattacharya, P. and Kumar, J. (2016), "Uplift capacity of anchors in layered sand using finite element limit analysis: Formulation and results", *J. Geomech.*, **16**(3), 04015078.
DOI: 10.1061/(ASCE)GM.1943-5622.0000560, 04015078

Bhattacharya, P. and Roy, A. (2016), "Improvement in horizontal capacity of anchor plate in clay by granular column", *Geomech. Eng.*, **10**(5), 617-633.

Bildik, S., Laman, M. and Suleinman, M.T. (2013), "Uplift behavior of anchor plates in slope", *Geo-Congress 2013*, San Diego, California, U.S.A., March.

Bottero, A., Negre, R., Pastor, J. and Turgeman, S. (1980), "Finite element method and limit analysis theory for soil mechanics problems", *Comput. Methods Appl. Mech. Eng.*, **22**(1), 131-149.

Bouazza, A. and Finlay, T.W. (1990), "Uplift capacity of plate anchors buried in a two-layered sand", *Geotechnique*, **40**(2), 293-297.

Das, B.M. and Seeley, G.R. (1975), "Breakout resistance of shallow horizontal anchors", *J. Geotech. Engrg. Div.*, **101**(9), 999-1003.

Davis, E.H. (1968), *Theories of Plasticity and Failure of Soil Masses in Soil Mechanics: Selected topics*, Elsevier, New York, U.S.A., pp. 341-354.

Dickin, E.A. (1988), "Uplift behavior of horizontal anchor plates in sand", *J. Geotech. Eng.*, **114**(11), 1300-

1317.
Keskin, M.S. (2015), "Model studies of uplift capacity behaviour of square plate anchors in geogrid-reinforced sand", *Geomech. Eng.*, **8**(4), 595-613.
Khatri, V.N. and Kumar, J. (2011), "Effect of anchor width on pullout capacity of strip anchors in sand", *Can. Geotech. J.*, **48**(3), 511-517.
Kumar, J. (1997), "Upper bound solution for pullout capacity of anchors on sandy slopes", *J. Numur. Anal. Methods Geomech.*, **21**(7), 477-484.
Kumar, J. (2001), "Seismic vertical uplift capacity of strip anchors", *Geotechnique*, **51**(3), 275-279.
Kumar, J. (2003), "Uplift resistance of strip and circular anchors in a two layered sand", *Soils Fdns*, **43**(1), 101-107.
Kumar, J. and Khatri, V.N. (2008), "Effect of footing width on bearing capacity factor N_γ for smooth strip footings", *J. Geotech. Geoenviron. Eng.*, **134**(9), 1299-1310.
Kumar, J. and Kouzer, K.M. (2008), "Vertical uplift capacity of horizontal anchors using upper bound limit analysis and finite elements", *Can. Geotech. J.*, **45**(5), 698-704.
Lyamin, A.V. and Sloan, S.W. (2002), "Lower bound limit analysis using non-linear programming", *J. Numur. Methods Eng.*, **55**(5), 573-611.
Merified, R.S. and Sloan, S.W. (2006), "The ultimate pullout capacity of anchors in frictional soils", *Can. Geotech. J.*, **43**(8), 852-868.
Merifield, R.S., Lyamin, A.V. and Sloan, S.W. (2006), "Three dimensional lower-bound solutions for the stability of plate anchors in sand", *Geotechnique*, **56**(2), 123-132.
Meyerhof, G.G. (1973), "Uplift resistance of inclined anchors and piles", *Proceedings of the 8th International Conference on Soil Mechanics and Foundation Engineering*, Moscow, Russia, August.
Meyerhof, G.G. and Adams, J.I. (1968), "The ultimate uplift capacity of foundations", *Can. Geotech. J.*, **5**(4), 225-244.
Murray, E.J. and Geddes, J.D. (1987), "Uplift of anchor plates in sand", *J. Geotech. Eng.*, **113**(3), 202-215.
Murray, E.J. and Geddes, J.D. (1989), "Resistance of passive inclined anchors in cohesionless medium", *Géotechnique*, **39**(3), 417-431.
Niroumand, H. and Kassim, K.A. (2014a), "Uplift response of circular plates as symmetrical anchor plates in loose sand", *Geomech. Eng.*, **6**(4), 321-340.
Niroumand, H. and Kassim, K.A. (2014b), "Experimental and numerical modeling of uplift behavior of rectangular plates in cohesionless soil", *Geomech. Eng.*, **6**(4), 341-358.
Niroumand, H. and Kassim, K.A. (2014c), "Square plates as symmetrical anchor plates under uplift test in loose sand", *Geomech. Eng.*, **6**(6), 593-612.
Ovesen, N.K. (1981), "Centrifuge tests on the uplift capacity of anchors", *Proceedings of the 10th International Conference on Soil Mechanics and Foundation Engineering*, Stockholm, Sweden, June.
Rangari, S.M., Choudhury, D. and Dewaikar, D.M. (2013), "Seismic uplift capacity of shallow horizontal strip anchor under oblique load using pseudo-dynamic approach", *Soils Found.*, **53**(5), 692-707.
Rao, K.S.S. and Kumar, J. (1994), "Vertical uplift capacity of horizontal anchors", *J. Geotech. Eng., ASCE*, **120**(7), 1134-1147.
Rowe, R.K. and Davis, E.H. (1982), "The behavior of anchor plates in sand", *Geotechnique*, **32**(1), 25-41.
Sakai, T. and Tanaka, T. (2007), "Experimental and Numerical study of uplift behavior of shallow circular anchor in two-layered sand", *J. Geotech. Geoenviron. Eng.*, **133**(4), 469-477.
Sloan, S.W. (1988), "Lower bound limit analysis using finite elements and linear programming", *J. Numur. Anal. Methods Geomech.*, **12**(1), 61-77.
Sloan, S.W. (2013), "Geotechnical stability analysis", *Geotechnique*, **63**(7), 531-572.
Yu, S.B., Merifield, R.S., Lyamin, A.V. and Fu, X.D. (2014), "Kinematic limit analysis of pullout capacity for plate anchors in sandy slopes", *Struct. Eng. Mech.*, **51**(4), 565-579.

CC